International Journal of Scientific Research in Engineering and Management (IJSREM)
Volume: 10 Issue: 10 | Oct - 2026 SJIF Rating: 8.659 ISSN: 2582-3930

A Single-Stage Bridgeless PFC Charger with Enhanced Power Quality for LEV-Mounted Solar PV Panels

S. Anusha [1] G.P. Merinle[2], Rambabu.Yerra[3], T. Rajeswari[4]

[1]Electrical and Electronics Engineering & Holy Mary Institute of Technology and Science
[2]Electrical and Electronics Engineering & Holy Mary Institute of Technology and Science
[3]Electrical and Electronics Engineering & Holy Mary Institute of Technology and Science
[4]Electrical and Electronics Engineering & Holy Mary Institute of Technology and Science

---

Abstract - Researchers are investigating strategies to integrate solar photovoltaic (PV) with electric vehicles (EVs) as both sectors gain popularity for long-term growth sustainability. One emerging business is the installation of solar panels on light-electric vehicles (LEV). The literature on onboard charging techniques with integrated grid and solar PV input for an LEV-mounted PV panel is sparse and leaves much to the imagination. This paper proposes a PFC (power factor corrected) charger that focuses on the same. It features a three-port topology which connects to the grid, PV panels and batteries. The battery can be charged together with the grid or independently by the PV panels. Its declared aim is to simplify the design and at the same time improve the total harmonic distortion (THD) of the source current to fulfil the requirements of the IEC 61000-3-2 standard. In the design of the controller for each input, PSIM software uses small-signal modelling with ac-sweep analysis. To eliminate disturbances in the output of steady-state PV system, a variable step size maximum power point tracking (MPPT) technology is utilised. It is designed to operate at best even under dynamically challenging conditions such unpredictable power input interruptions, large variations in output power demand and sudden variations in grid voltage. As a demonstration of the charger's functionality, we constructed a lab prototype capable of delivering 500 W output power and 1.2% total harmonic distortion (THD) in grid current.

Key Words The acronyms LEV, MPPT, PFC, PV, and THD stand for light electric vehicle, power factor correction, solar photovoltaic, and overall harmonic distortion, respectively.

1.INTRODUCTION

New study possibilities have been opened up by the increasing popularity of light electric vehicles (LEVs) equipped with photovoltaic (PV) panels. This trend is especially noticeable in developing nations like India. Electric vehicle (EV) charging infrastructure is a hotspot for innovation. For completely grid-dependent EVs, numerous power factor-corrected (PFC) chargers have been suggested in the last several decades [1, 2, 3, 4, 5, 6, 7]. Remarkably, these arrangements are categorised as either single-stage [1], [2], [3], [4] or two-stage [5], [6], [7] chargers according to their design. The basic idea behind a pulse-free charger (PFC) is to keep the input power factor high and to provide the battery with a current that does not ripple. To achieve both of these goals, two-stage topologies require ac-dc and dc-dc converters. In single-stage charging, nevertheless, a single ac-dc interfacing converter handles both tasks. Now it has the inherent advantage of being more efficient and having a less complicated structure [1]. A two-stage onboard charger often uses galvanic isolation in the second stage, where an isolated dc-dc converter is incorporated. To be clear, transformers are not an absolute necessity for electric vehicle safety according to the SAE J1772 standard. It is also unnecessary to offer isolation with grid input because the battery ground is always floating with the vehicle chassis [8, 9], [10]. As an alternative to the cumbersome transformer, smaller and less expensive relay circuits can be used for safety purposes [10]. Also, the size, losses, complexity, and switch stress caused by leakage inductance are all increased when transformers are integrated into isolated topologies. Therefore, as a result of their low cost, non-isolated single-stage topologies are quickly becoming the preferred charging solution for LEVs.

The sinusoidal current shaping of grid input is often accomplished using a PFC architecture that is based on a boost converter [11]. The output voltages are higher than the peak grid voltage, which limits their use for single-stage low-voltage charging applications. Other topologies that can handle buck-boost, like Cuk, SEPIC, and Zeta, are great choices for these kinds of applications [12]. Topologies derived from Cuk converters provide a number of advantages over the others, such as offering continuous current at both the input and the output and native protection against inrush current. The cascade of a diode-bridged rectifier (DBR) and a Cuk converter forms a traditional bridged Cuk rectifier [13]. The conduction losses in DBR, however, have a negative impact on charger efficiency. As an alternative to the bridged Cuk topology, several bridgeless Cuk topologies have been suggested (see references 14, 15, 16, 17, and 18) for the purpose of improving efficiency. To avoid the usage of a bridge, the PFC rectifier described in [14] makes use of two Cuk circuits that operate in opposite voltage polarities. It makes more components and uses less of each component. Researchers in [15] and [16] used a single Cuk circuit to handle both positive and negative voltage polarity, which reduced the number of components. In order to decrease the size of the output capacitor, a novel control mechanism is

utilised in [15]. Improved efficiency in [16] also requires an additional regulated switch. In [17], the authors offer a bridgeless Cuk PFC architecture that uses soft switching to achieve full voltage and load capacity. Implementing soft switching requires more passive components and semiconductor devices, but it improves efficiency by lowering switching and conduction losses. Unfortunately, these bridgeless PFC topologies only support charging through grid input for their single stage. As a result, in order to achieve maximum power point tracking (MPPT) with a PV panel that has an LEV, an extra dc-dc converter would be necessary [19]. Typical charging topologies are shown in a block diagram [20],

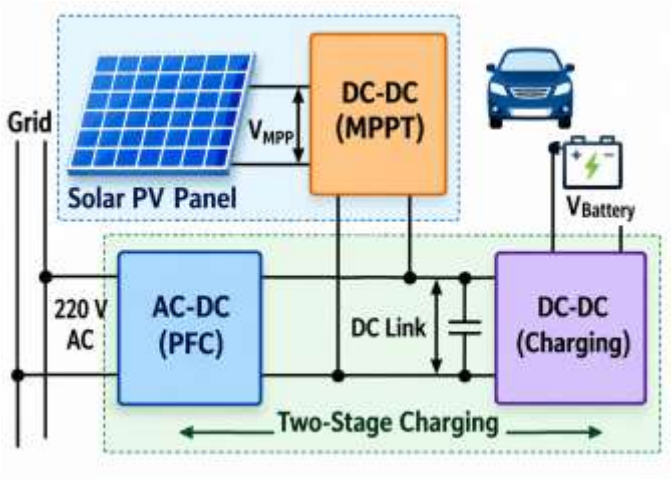


Fig. 1. Standard photovoltaic (PV) systems with a built-in PFC charging mechanism

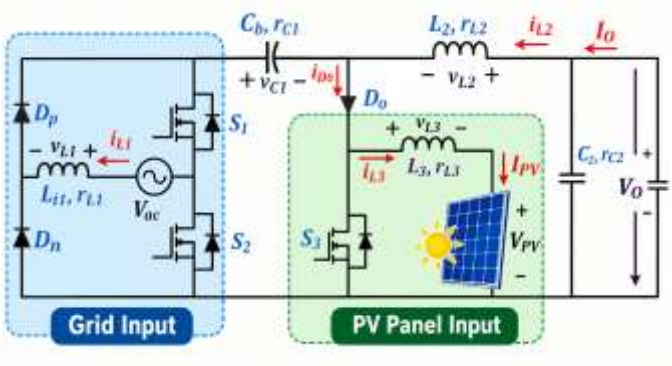


Fig. 2. Schematic of bridgeless LEV charger.

Figure 1 depicts a dual input source that incorporates both grid and PV panel input, as described in references [21], [22], and [23]. Clearly, the necessary charging configuration is achieved by use of three converters. At the PV panel end, a dc-dc converter executes the MPPT operation, and another dc-dc converter is used for charging the batteries. An ac-dc converter is used for power factor correction in this setup. For high-power output, this kind of setup is typical. Nevertheless, a plethora of magnetic and switching components are required. To avoid this issue, an alternate configuration that does not use a dc-dc converter to conduct the MPPT is proposed in [24]. Here, a photovoltaic panel is connected directly to the DC line, without the need for an interface converter. In this setup, the PFC converter is running in boost mode, hence the PV panels need to be able to handle a greater voltage at the MPP. A multiport charger is another option for simultaneously connecting numerous sources with fewer parts [25]. Power from photovoltaic panels and standard household outlets are both compatible with this apparatus. Using a single power converter for all processes enhances efficiency and minimises cost. But it's limited to using just one power source simultaneously. In [26], a Z-source inverter is used to create a multiport PFC charger that converts electricity in a single stage. Having said that, more switching components are needed. Rare is the multi-input PFC charger that can simultaneously and independently activate all sources with a reduced number of components. Figure 2 shows a bridgeless dual-input LEV charger that was developed by Cuk in order to solve the problems mentioned earlier. The PV panel is the secondary input in this case, whereas the grid is the primary one. To accommodate an additional source, a standard bridgeless Cuk charger is enhanced with an additional switch and inductor.

2. System Configuration and Operation Principles

This article describes a bridgeless multiport PFC charger that operates on the same concept as a standard Cuk PFC rectifier and inherits all of its characteristics. Beyond that, a standard two-port Cuk converter can easily accommodate the PV panel input. Figure 2 depicts the updated design incorporating three inductors and two capacitors. Three diodes and three switches are also required. Swapping out two DBR diodes for two switches, S1 and S2, allows for the realisation of the bridgeless architecture for ac input. In a positive voltage polarity, diode Dp conducts and in a negative voltage polarity, diode Dn does the same. depicts the real-time application of a sinusoidal grid voltage to the main input,

$$V_{ac}(t) = V_p \sin(314t). \qquad (1)$$

Vp stands for the maximum value of Vac(t) in the previous equation. We may assume Vac(t) is constant and represent it as Vac in a single switching cycle because the switching frequency is comparatively high compared to the grid frequency. Just as DS1 and DS2 in a switching period indicate the time-varying duties of grid input and PV input, respectively, so may DS1(t) and DS2(t). It is DS1's job to regulate switches S1 and S2. Along with the other two switches, DS2 operates switch S3 to carry out the maximum power point tracking (MPPT) of the PV panel input. Depending on the availability of each source, the charger functions in one of three charging states: grid charging, PV stand-alone, or dual input charging. I. Charging from Two Sources A PV system and the grid can work together to charge batteries through dual input charging. In order to show how the charger works throughout one switching cycle for grid-PV charging, three different modes are utilised. The reasoning that was used

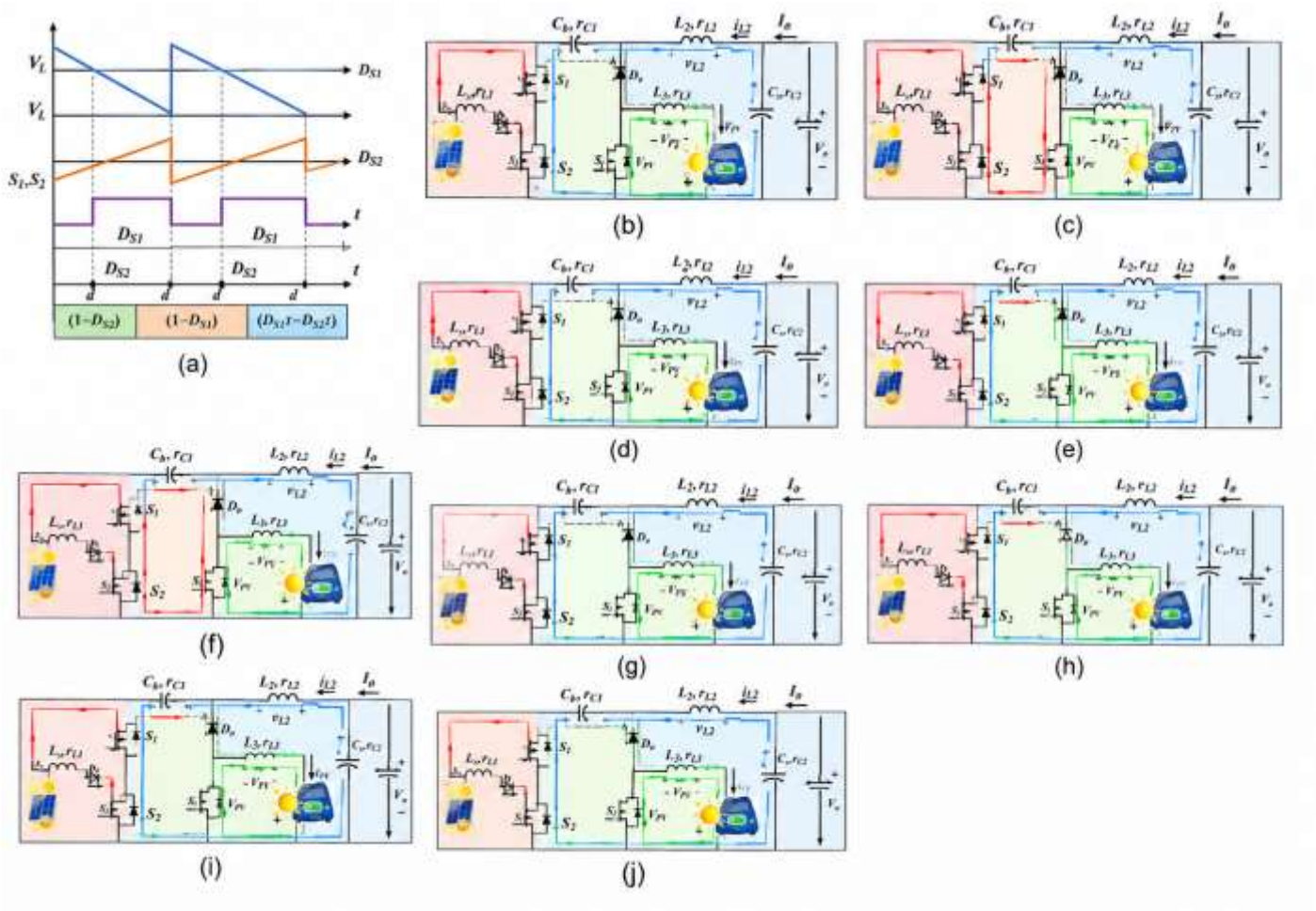


Fig. 3(a) For each operating mode, a graphical representation of the switching pulse generation is provided. The following circuit representations are equivalent: (b)–(d) for positive voltage polarity dual input charging, (e)–(g) for negative voltage polarity dual input charging, (h)–(i) for grid charging, and (j)–(k) for PV stand-alone charging.

The following circuit representations are equivalent: (b)–(d) for positive voltage polarity dual input charging, (e)–(g) for negative voltage polarity dual input charging, (h)–(i) for grid charging, and (j)–(k) for PV stand-alone charging. Figure 3(a) shows the process for producing control pulses for every mode. The durations of modes 1, 2, and 3 are represented here by d1, d2, and d3, respectively. Figure 3(b)-(d) shows the charger in action with a positive voltage polarity. Similarly, its operation for negative polarity is shown in Figure 3(e)-(g). Switches S1 and S2 are active in modes 1 and 3, whilst switch S3 is active in mode 3. When in mode 1, the grid charges the input inductor L1. Since iL1 flows through Dp and Dn is reverse biased when the voltage is positive. If the voltage polarity is negative, however, iL1 will flow through Dn. As a result, output inductor L2 is charged by C1. L3, the inductor, discharges through C1 at the PV input. On the second mode, L1 discharges due to iL1 flowing from diode Dp and switch S2 under positive voltage polarity. The opposite is also true for negative voltage: it goes through S1 and Dn. L3 can now be charged via the input of PV panels because S3 is turned on. L1 and L2, the other two inductors, also discharge in this mode for both positive and negative voltages.

Mode 3: Here, iL1 and iL2 can continue along the same route as in Mode 1, since the switching states of S1 and S2 are identical. In mode 3, the only change is that inductor L3 is charged and switch S3 is turned on. One way to express the voltage conversion ratio of each input to each output is by balancing the voltage of each inductor with respect to time.

$$\frac{V_o}{V_{ac}} = \frac{D_{S1}}{1 - D_{S1}} \text{ and } \frac{V_o}{V_{PV}} = \frac{D_{S1}}{1 - D_{S2}}. \quad (2)$$

For a broad range of loads, the switch current iS3 is negative at the start of mode 2, but it switches to positive in mode 3. When mode 2 begins, its magnitude is big enough to discharge S3's output capacitance and produce the zero-voltage switching (ZVS) state across a wide range of loads. A fixed turn-on delay mechanism is used for the ZVS turn-on of S3 since it is simple to implement. There are two modes of operation for power transfer when using the proposed converter for grid charging; this is because it is functionally identical to a standard PFC Cuk charger. The converter is shown operating in modes 1 and 2, respectively, in Figure 3(h) and (i). In modes 1 and 2, the switches S1 and S2 are switched on and off, respectively, while S3 is

conducted in both modes. Mode 1 also involves charging inductors L1 and L2 and discharging capacitor C1. The second method also involves C1 charging and L1 and L2 discharging.

C. Charging from PV Systems Alone The converter that is being showcased can collect solar energy regardless of whether you are driving or parked by the side of the road. Figures 3(j) and (k) show what is referred to as PV stand-alone charging. Solar panels use a capacitor as a middleman to transmit energy from the panel to the output. Aside from constantly running S1 and S2, there are only two modes of operation for this. In each mode, S3 is switched. In Fig. 3(k), we can see the circuit setup for mode 2. Modus 2 disables switch S3.

TABLE I

SYSTEM SPECIFICATIONS

Specifications	Parameters	Value (Range)
AC Mains	Voltage (V_{ac})	110 V (90 V-130 V)
	Power (P_{ac})	470 W (P_{max} = 570 W)
PV Panel	Voltage at MPP (V_{pv})	40 V
	Power at MPP (P_{pv})	121.48 W
Output	Voltage (V_o)	72V (63 V-87 V)
	Power (P_o)	470 W (P_{max} = 570 W)
Switching Freq.	-	20 kHz

3.The Development of an Electric Vehicle Discharger

The charger's comprehensive design equations. The charger is engineered to function in continuous conduction mode (CCM) in accordance with the system requirements listed in Table I. In a fully drained condition, the output voltage of the battery charger is lower than 87 V (Vo,max), and vice versa; a fully charged state, the output voltage is higher than 63 V (Vo,min). Almost linearly related to the output voltage is the charger's output power, which fluctuates somewhat. Its intended use is to manage grid voltage spikes up to 130 V (Vac,max) and sudden drops down to 90 V (Vac,min). Therefore, every inductor and capacitor should be designed to operate in CCM for all critical working conditions, including (Vac,min, Vo,min), (Vac,min, Vo,max), (Vac,max, Vo,min), L1 is the input inductor, which has a significant impact on input current total harmonic distortion (THD) in a CCM design. As a result, it is engineered to operate with the current ripple as low as possible. Keep in mind that when the grid voltage is greatest, you get the critical value of L1. The supplied design equation is for the same.

$$L_1 = \frac{D_{S1}}{\gamma_{L1} f_s}\frac{V_{ac}^2}{P_{ac}} = \frac{V_{ac,max}^2}{\gamma_{L1} f_s}\frac{V_{o,max}/P_{ac,max}}{V_{o,max} + \sqrt{2}V_{ac,max}}. \quad (3)$$

Computed value of L1 from (3) is 6.0 mH, and the chosen value for prototype development is also same with an 8% current ripple (γL1) at input. The expression for the calculation of L2 can be written as

$$L_2 = \frac{1 - D_{S1}}{\gamma_{L2} f_s}\frac{V_o}{i_{L2}} = \frac{V_{o,max}}{\gamma_{L2} f_s i_{L2}}\frac{\sqrt{2}V_{ac,max}}{V_{o,max} + \sqrt{2}V_{ac,max}}. \quad (4)$$

It is noteworthy that an optimal value of L2 is attained at peak grid voltage and maximum output voltage. It has an inverse relationship with current (iL2) flowing through it. Following equation can be used to compute the instantaneous value of (iL2) under a specified conditions (Vac,max and Vo,max):

$$i_{L2}(t) = \frac{P_{ac} - P_{ac}\cos(2\omega t)}{V_o} = \frac{2P_{ac,max}}{V_{o,max}}. \quad (5)$$

The expression for determining L2 for an aforementioned critical circumstance is as follows:

$$L_2 = \frac{V_{o,max}^2}{\gamma_{L2} f_s}\frac{((\sqrt{2}V_{ac,max})/(2P_{ac,max}))}{V_{o,max} + \sqrt{2}V_{ac,max}}. \quad (6)$$

The calculated and chosen value of L2 for 15% current ripple (γL2) is 1.5 mH. The input inductor (L3) at PV panel

TABLE II

EXPERIMENTAL COMPONENT RATING

Device	Rating
Grid Input Inductor (L_1)	6 mH, ESR(r_{L1})=0.26 Ohm
Output Inductor (L_2)	1.5 mH, ESR(r_{L2})=0.13 Ohm
PV Input Inductor (L_3)	4.8 mH, ESR(r_{L3})=0.2 Ohm
Intermediate Capacitor (C_1)	5 μF
DC Link Capacitor (C_2)	6.6 mF

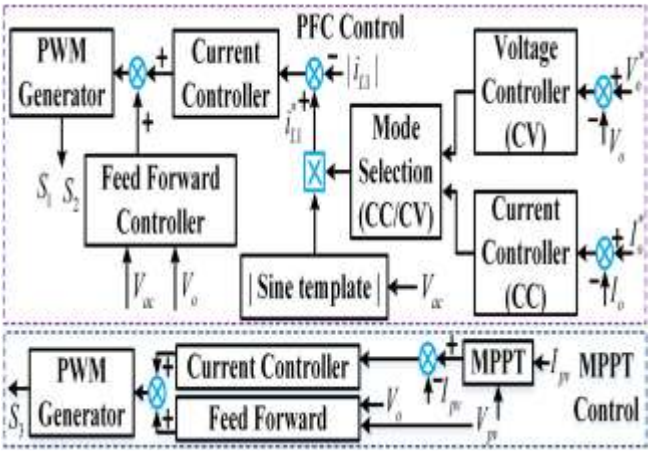


Fig. 4. Approach to controlling a bridgeless electric vehicle charger.

input is mostly determined by PV power, but it is also controlled by grid voltage since it impacts duty ratio DS2.Following equation is used to compute the critical value of L3 for 12% current ripple (γL3):

$$L_3 = \frac{D_{S2} V_{pv}^2}{\gamma_{L3} f_s P_{pv}} = \frac{V_{pv}^2 / P_{pv}}{\gamma_{L3} f_s} \left(1 - \frac{V_{pv}}{V_{o,max} + \sqrt{2} V_{ac,max}}\right). \quad (7)$$

From aforementioned expression, the computed and selected value of L3 are 4.7 and 4.8 mH, respectively.

B. Design of C1 and C2 in CCM

Grid input current has a significant impact on the value of the intermediate capacitor (C1). The critical value of C1 is derived for maximum grid power, as illustrated in C1 design equation here

$$C_1 = \frac{(1 - D_{S1}) I_{L1}}{\lambda_{C1} f_s V_{C1}} = \frac{1}{\lambda_{C1} f_s} \frac{2 P_{ac,max}}{(V_{o,max} + \sqrt{2} V_{ac,min})^2}. \quad (8)$$

To achieve 30% voltage ripple (λC1) at the specified condition, an optimal value of C1 is determined to be 4.14 µF and the selected value for prototype development is 5 µF. The purpose of output capacitor (C2) is to absorb the second harmonic component of battery current. It can be stated as

follows:

$$C_2 = \frac{I_o}{2\omega \lambda_{C2} V_o} = \frac{P_o}{2\omega \lambda_{C2} V_o^2} = \frac{P_{o,max}}{2\omega \lambda_{C2} V_{o,max}^2}. \quad (9$$

For a 2% ripple (λC2), computed and selected values for C2 are 6 and 6.6 mF, respectively. Selected values of the components based on calculations and system parameters are summarized in Table II.

3.1. Power factor-corrected (PFC) charger presented and PFC Chargers Work

A Power Factor-Corrected (PFC) charger is an electronic device featuring an AC-DC converter that ensures the electrical current it draws aligns perfectly with the input voltage, pushing the power factor close to 1.0. This prevents grid harmonic distortion, improves energy efficiency, and complies with international power quality standards.

Standard diode rectifiers draw current in harsh, short pulses, which creates harmonic distortion and wastes energy. A PFC circuit uses high-frequency switching and control loops to force the current waveform to follow the voltage waveform, mimicking a purely resistive load.

4.Simulation Results and Discussion

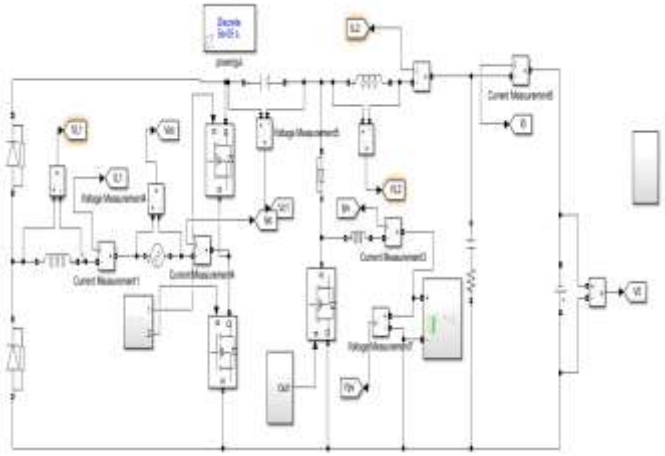


Fig.5. MATLAB/Simulink circuit diagram

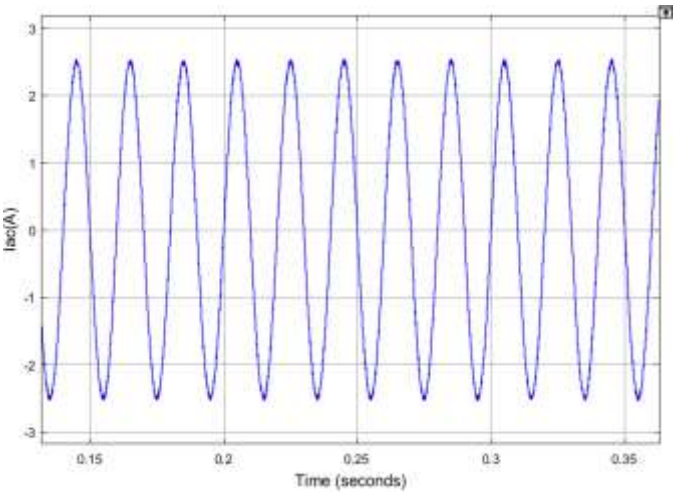


Fig.6. AC current waveform

The given graph represents the AC current waveform (\(I_{ac}\)) with respect to time, likely obtained from a MATLAB/Simulink simulation of a power-electronic converter or an AC power system.

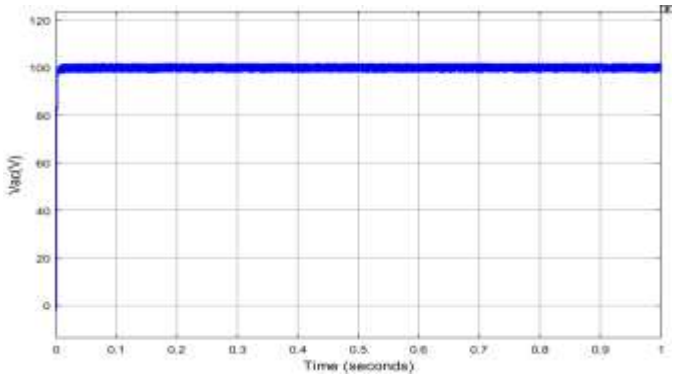


Fig.7.The given graph represents the DC voltage

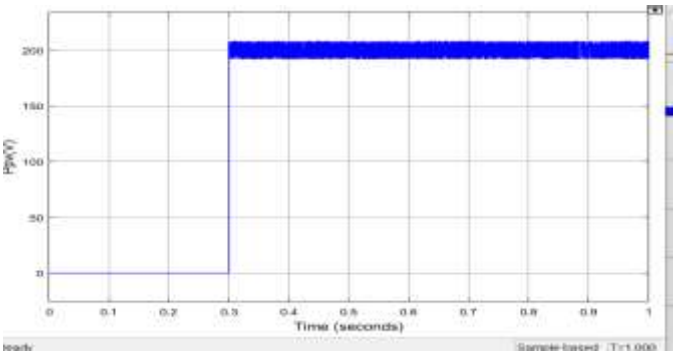


Fig.8.The graph shows the photovoltaic (PV) panel output voltage versus time.

Obtained from a MATLAB/Simulink simulation. It illustrates the initial startup period and the voltage maintained by the PV system during steady-state operation.

3. CONCLUSIONS

The proposed **single-stage bridgeless PFC charger** successfully enhances the charging performance of **Light Electric Vehicles (LEVs)** by combining high-efficiency power conversion with improved power quality. Eliminating the conventional diode bridge reduces conduction losses, resulting in higher overall efficiency. The integrated Power Factor Correction enables the charger to achieve a power factor close to unity while maintaining current THD within international standards. The incorporation of a solar PV panel allows the battery to utilize renewable energy, reducing dependence on the utility grid and lowering operating costs. Overall, the proposed system offers a compact, efficient, environmentally friendly, and reliable charging solution suitable for next-generation electric mobility.

A grid and PV panel interfaced charger for LEV is presented in this article with the merit of improved PQ of grid current. The dc output power is generated from both sources, capable of operating simultaneously and separately. A small signal analysis, which is further verified by ac-sweep in PSIM, is performed for the frequency response of the designed charger. It improves the PQ of ac current and MPPT of PV panel input under steady-state as well as dynamic operational conditions. Few components are shared between each source to reduce the overall components. An inductor at each input eliminates the necessity of a large filter. The charger configuration gives an additional benefit over conventional topologies by improving THD in grid current for dual input operation. Here, addition of a PV panel reduces the THD by improving the voltage profile of common intermediate capacitor between two sources. Operation of the presented topology is verified on a 500 W laboratory prototype under steady-state and diverse dynamic conditions.

REFERENCES

[1] T.-T. Le, R. M. Hakim, and S. Choi, “A high-efficiency bidirectional single-stage AC–DC converter under wide voltage range for fast chargers,” IEEE Trans. Power Electron., vol. 38, no. 4, pp. 4945–4956, Apr. 2023.

[2] H. Nazi, E. Babaei, S. Tohidi, and M. Liserre, “An isolated SRC-based single phase single stage battery charger for electric vehicles,” IEEE Trans. Transport. Electrific., vol. 9, no. 1, pp. 1252–1262, Mar. 2023.

[3] H. Kim, J. Park, S. Kim, R. M. Hakim, H. Belkamel, and S. Choi, “A single-stage electrolytic capacitor-less EV charger with single- and three-phase compatibility,” IEEE Trans. Power Electron., vol. 37, no. 6, pp. 6780–6791, Jun. 2022.

[4] B. Vardani and N. R. Tummuru, “A single-stage bidirectional inductive power transfer system with closed-loop current control strategy,” IEEE Trans. Transport. Electrific., vol. 6, no. 3, pp. 948–957, Sep. 2020.

[5] S. R. Meher and R. K. Singh, “A standard two stage on board charger with single controlled PWM and minimum switch count,” IEEE Trans. Ind. Appl., vol. 59, no. 4, pp. 4628–4639, Jul./Aug. 2023.

[6] A. Singh, J. Gupta, and B. Singh, “Design and control of two stage battery charger for low voltage electric vehicles using high gain buckboost PFC AC–DC converter,” IEEE Trans. Ind. Appl., vol. 59, no. 5, pp. 6125–6135, Sep./Oct. 2023.

[7] M. Tong, M. Cheng, S. Wang, and W. Hua, “An on-board two-stage integrated fast battery charger for EVs based on a five-phase hybrid excitation flux-switching machine,” IEEE Trans. Ind. Electron., vol. 68,
no. 2, pp. 1780–1790, Feb. 2021.

[8] C.-Y. Oh, D.-H. Kim, D.-G. Woo,W.-Y. Sung, Y.-S. Kim, and B.-K. Lee, “A high-efficient nonisolated single-stage on-board battery charger for electric vehicles,” IEEE Trans. Power Electron., vol. 28, no. 12, pp. 5746–5757, Dec. 2013.

[9] A. V. J. S. Praneeth and S. S. Williamson, “Modeling, design, analysis, and control of a nonisolated universal on-board battery charger for electric transportation,” IEEE Trans. Transport. Electrific., vol. 5, no. 4, p. 912–924, Dec. 2019.